T3.5-P49

Signal Classification Using Covariance Matrices: A Riemannian Geometry Framework

Shaelyn G. Divins‡, Joshua S. Beard†, Oluwaseun Winsala*, Maxwell Ble*, Anthony O. Smith*, Adrian M. Peter*, Dean Clauter¥

‡Elizabethtown College, †Seattle University, *Florida Institute of Technology, ¥Air Force Technical Applications Center

This material is based upon work/research supported in part by the National Science Foundation under Grant No. 1263011 and 1560345.

Abstract

We present a novel framework for time series classification that leverages the geometric structure of covariance matrices when labeling signals. Our method maps each signal to a new multivariate localized feature signal (MLFS) representation, from which we compute a covariance descriptor. This robust MLFS covariance representation handles classification tasks where the *sampling rates of the signals vary within a class, and across classes*. We demonstrate that simply using the k-nearest neighbor classification rule with the Riemannian metric between the MLFS covariance matrices produces state-of-the art results on a number of standard datasets. Moreover, for the first time, we showcase results on the full Library of Typical Infrasonic Signals dataset which contains four categories of infrasound observations.

MLFS Covariance Descriptor

Figure 1 illustrates our approach which maps each input signal (top left) to a multivariate localized feature signal (MLFS) covariance descriptor (far right). The dynamics of a signal are captured by extracting per-window feature vectors and then looking at the temporal signature across each feature dimension. The resulting time series, per feature dimension, are then used to estimate a covariance matrix that encodes all pairwise correlations between feature dimensions. Our k-NN classification algorithm uses the Riemannian metric between covariance matrices to classify the signals.

We extracted the following features: identity map (returns the signal), instantaneous frequency (IF)[1], derivatives (first and second order), local statistics (standard deviation, skewness, kurtosis) , local binary pattern (LBP)[2], and stationary wavelet transform (SWT)[3].

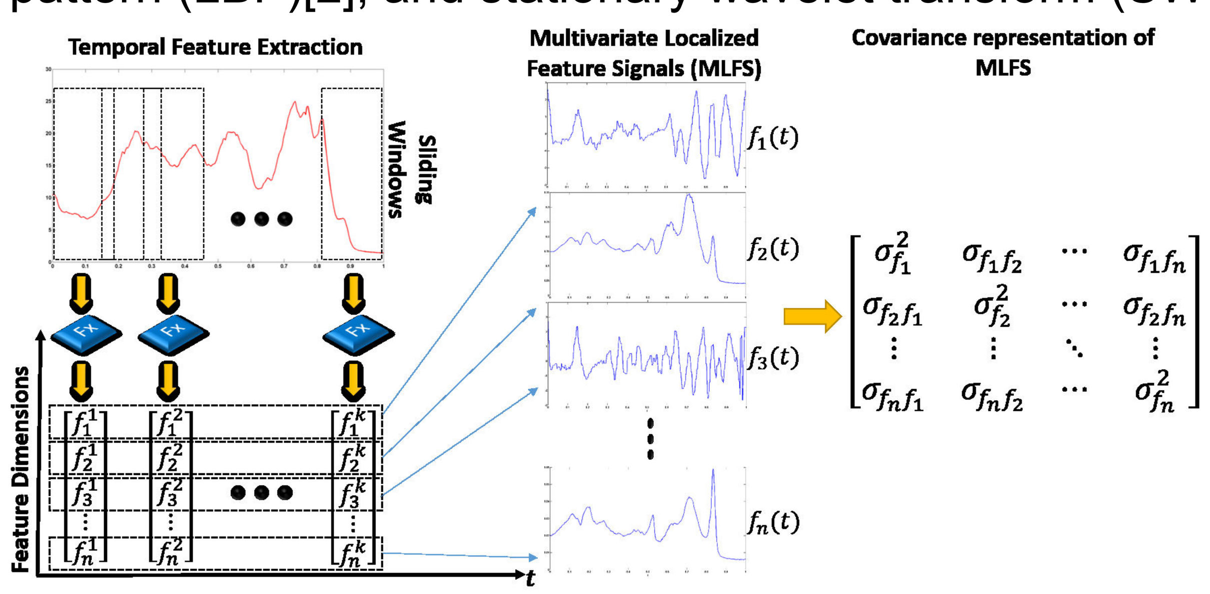

Figure 1

Experiments

In Table 1 the columns 2–5 reflect the previous state-of-the-art accuracies as reported in [4]. Results using dynamic time warping (DTW) , and 'Warping Window' which has been abbreviated as 'WW'. Our MLFS covariance descriptor k-NN classifier accuracies are in the last column. We outperform the other methods on half of the UCR datasets by significant amounts.

	Dataset (# classes)	*Euclidean 1-NN(%)*	*DTW 1-NN(%)*	*DTW 1-NN best WW(%)*	*Feature-based linear (%)*	*MLFS k-NN (%)*
UCR	Beef (5)	53.3	50.0	53.3	56.7	**83.3**
	Adiac (37)	61.1	60.4	60.9	64.5	**72.6**
	Lightning-7 (15)	57.5	72.6	71.2	56.2	61.6
	50 Words (50)	63.1	69.0	**75.8**	54.7	43.0
	FaceAll (14)	71.4	80.8	**80.8**	70.8	67.9
	OSU Leaf (6)	51.7	59.1	61.6	83.5	**87.6**
	Fish (7)	78.3	83.3	**84.0**	82.9	77.41
	Swedish Leaf (15)	78.9	79.0	84.3	77.3	**91.2**
	Yoga (2)	83.0	83.6	**84.5**	77.4	77.8
	Lightning-2 (2)	75.4	86.9	86.9	80.3	**88.9**

Table 1

Infrasound

Infrasound refers to acoustic frequencies below the audible range (typically < 20 Hz). Most commonly generated by natural and man-made sources to include atmospheric turbulence, aurora, lightning, bolides, explosions, volcanoes, and rockets. Since infrasound waves can potentially travel thousands of kilometers, they are considered vitally important for standoff monitoring of nuclear detonations. We evaluated the proposed classification method on four categories of infrasound waves, detailed below. The datasets had a variety characteristics (e.g. multichannel data with varying sample rates) that we were able to effectively manage in our framework. The multichannel data were aligned and a mean curve calculated from this we calculated the MLFS covariance descriptor.

MLFS Covariance k-NN Classification Accuracy: *83.6%* We anticipate the results will continue to improve with better features.

Auroral Waves

Waves generated in the upper atmosphere by the supersonic motions of large scale auroral electrojet during periods of intense geomagnetic disturbances at polar latitudes.

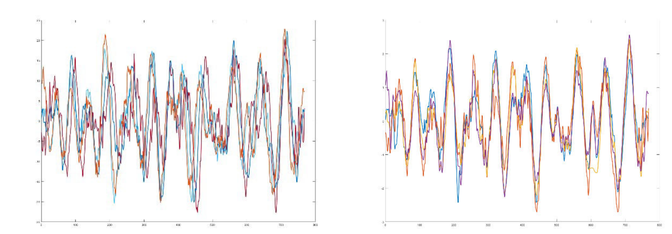

Original Aligned

Microbaroms Waves

Sea wave-are interaction at the surface during marine storms generate infrasonic waves.

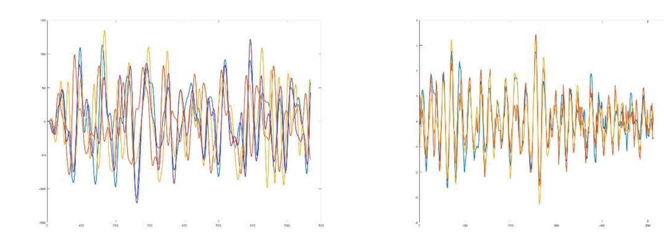

Original Aligned

Mountain Associated Waves

Atmospheric turbulence, generated by mountain ranges that interrupt the tropospheric wind flow.

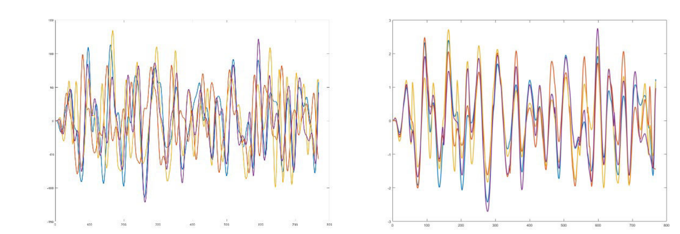

Original Aligned

Volcanic Waves

Produced by a volcanic eruption which is a sudden displacement of a very large air mass and of a rising cloud of hot gas.

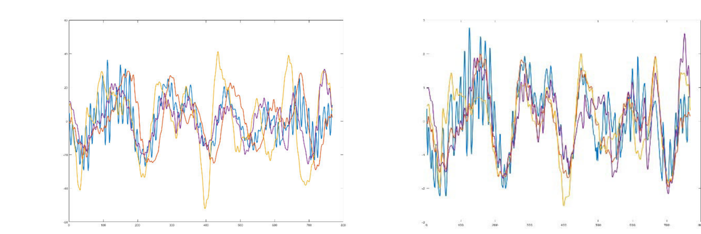

Original Aligned

Discussion

In half of the UCR datasets, our MLFS covariance descriptor approach achieves the highest accuracies—all by significant amounts over the competing methods. It is worth noting that, in the present work, we have only explored the use of 10 localized features. Whereas contemporary methods such as [4] optimized close to 1,000 possible features to produce their classification results. In their experiments, training on larger datasets took over eight hours. The longest run time for any of our datasets was on the order of a few minutes, for both training and testing together. The DTW method is able to achieve higher scores on some datasets largely due to the fact it non-linearly warps the signal. In this work, we detailed a new approach to signal classification framework that leverages the relational modeling strengths of covariance descriptors. In the future, we plan to investigate various other localized features and explore the use of other classification techniques like support vector machines that can be reformulated to work directly with covariance matrices. We will also evaluate on more infrasound datasets that are relevant to the nuclear monitoring mission.

Geometry of Matrices

A (non-degenerate) $n \times n$ covariance matrix is identifiable as an element of the set of symmetric positive definite (SPD) matrices, denoted P_n, which has the properties of a differential Riemannian manifold [5] (see Figure 2). Eq.(1) shows that this additional structure immediately allows us to carry out familiar calculus operations, like differentiation and integration, directly on this set. In the present context, we are interested in the following intrinsic Riemannian distance [6] between two SPD matrices C_1 and C_2 where, $\log(\cdot)$ is the principal matrix logarithm, $\|\cdot\|_F$ is the Frobenius norm, and λ_i's are the joint eigenvalues of $C_1^{-1}C_2$.

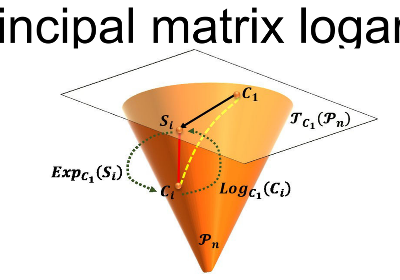

Figure 2

$$d(C_1, C_2) = \left\|\log\left(C_1^{-1}C_2\right)\right\|_F = \sqrt{\sum_{i=1}^{n} \log^2(\lambda_i)}, \quad \textbf{(1)}$$

References

1. L. Cohen, Time Frequency Analysis: Theory and Applications. Prentice Hall, 1994.
2. T. Ojala, M. Pietikainen, and T. Maenpaa, "Multiresolution gray-scale and rotation invariant texture classification with local binary patterns," IEEE Transactions on Pattern Analysis and Machine Intelligence, vol. 24, no. 7, pp. 971–987, July 2002.
3. G. Nason and B. Silverman, Wavelets and Statistics. Springer, 1995, ch. The Stationary Wavelet Transform and some Statistical Applications, pp. 281–299.
4. B. D. Fulcher and N. S. Jones, "Highly comparative feature-based time-series classification," IEEE Transactions on Knowledge and Data Engineering, vol. 26, no. 12, pp. 3026–3037, December 2014.
5. W. M. Boothby, An Introduction to Differentiable Manifolds and Riemannian Geometry. San Diego: Academic Press, 2002.
6. W. Förstner and B. Moonen, "A metric for covariance matrices," in Geodesy-The Challenge of the 3rd Millennium. Springer, 2003, pp. 299–309. [16] C. Wilson, J. Olson, and R. Richards, "Library of typical infrasonic signals," Report Prepared for ENSCO (subcontract no. 269343-2360.009), vol. 1, no. 4, 1996